Observable effects and peculiarities of the low-energy quantum gravity

Michael A. Ivanov
Physics Dept.,
Belarus State University of Informatics and Radioelectronics,
6 P. Brovka Street, BY 220027, Minsk, Belarus.
E-mail: ivanovma@tut.by.

Abstract

The existence of a background of ultra-strongly interacting gravitons is a key postulate of the author's low-energy gravity model. Side effects of the model due to photons interacting with this background may be important for cosmology, and their observation would be essential to support the model. The most important such effect is the quantum redshift mechanism, which may constitute an alternative to the generally accepted mechanism associated with the expansion of the universe. The model should have a weakening of the light flux due to a change in the number of photons, which replaces the influence of dark energy. Scattered photons may form a new background that can be detected by deep space missions. Some important predictions of the model are tested using observational data sets of SNe Ia, compact quasars and Lyman-alpha emitters. The article shows that the linear function $H(z)$ of the model satisfactorily describes the results of measurements of the Hubble parameter. Using a trial function for the weakening parameter, the possibility of a different interpretation of the Hubble tension is illustrated. The increasing angular diameter distance of this model is fitted to a set of 120 measurements of the angular sizes of compact quasars with redshifts of $0.46 - 2.76$ with independent calibration of their linear sizes. Attention is drawn to the possibility of a false interpretation of changes in the measured sizes of Lyman-alpha emitters observed by JWST in the redshift range of $3 - 7$ as evolutionary effects in the ΛCDM model, since these changes can be due to the increasing angular diameter distance of this model.

1 Introduction

The discoveries of the last decades in cosmology have an important feature: both dark matter and dark energy [1, 2] are something unknown that has been given a name. Intensive searches are underway for particles that could make up dark matter [3]; but it is not even clear where to look for the substance called dark energy. With the increase in the accuracy of measurements and the volume of cosmological surveys, some tensions with the standard cosmological model have appeared, for example, the Hubble tension, forcing one to assume the dynamic nature of dark energy [4, 5].

Attempts to construct a quantum theory of gravity based on Einstein's metric theory have been persistent for decades, but so far without success. Existing testable predictions of such models are few, since the main effects are expected to occur at Planck energies and distances [6]. In the author's model of low-energy quantum gravity, based on the postulate of the existence of a background of superstrongly interacting gravitons, the situation is different [7, 8, 9]. The model predicts small effects due to the interaction of photons with this background, which may be of great importance for cosmology. The most important of these is the quantum redshift mechanism, which may become an alternative to the mechanism based on the expansion of the universe. The second effect is due to non-head-on collisions of photons with background gravitons and leads to an additional weakening of the light flux from a distant source, making dark energy unnecessary. The scattered photons should create a new isotropic background, which will be the third effect. Multiple collisions of gravitons with each other should lead to the appearance of a sea of massive virtual gravitons with very low energies, which can pretend to be dark matter particles. The implications of these effects and their differences from the cosmological ΛCDM model are discussed here.

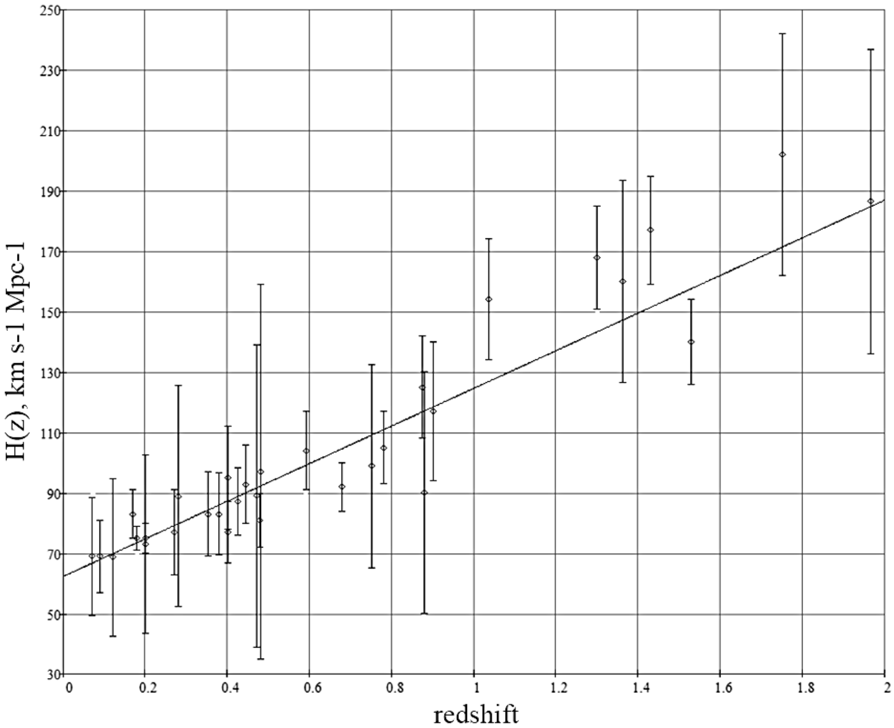

Figure 1: The fitting linear curve with $H_0 =< H_0 >$ (solid) and 32 observed points $H(z)$ from [10].

2 The Hubble parameter

In this model, the geometric distance r depends on the redshift z as:

$$r(z) = \frac{H_0}{c} \cdot ln(1+z), \tag{1}$$

where H_0 is the Hubble constant, which can be calculated in this model and has the following theoretical value: $H = 66.875\ km \cdot s^{-1} \cdot Mpc^{-1}$, c is the speed of light. The Hubble parameter $H(z)$ in this model without expansion can be defined as [7]:

$$H(z) \equiv \frac{dz}{dr} \cdot c = H_0 \cdot (1+z), \tag{2}$$

which is significantly different from its nonlinear dependence on redshift in ΛCDM. To compare this expression with observations, I have used a set of 32 observed points $H(z)$ from [10] obtained with the cosmic chronometers method and have calculated $< H_0 >$ and σ_{H_0} as described in [7, 11]. The obtained result: $< H_0 > \pm\sigma_{H_0} = 62.315 \pm 5.84$ has a high C.L. 98.80%; this means that the measurement accuracy of $H(z)$ does not allow us to distinguish between this model and ΛCDM. Fig. 1 shows the fitting curve with $H_0 =< H_0 >$ (solid) and observed points $H(z)$. The authors of the paper [10] estimated the Hubble constant in ΛCDM higher using the same data set: $< H_0 > \pm\sigma_{H_0} = 66.5 \pm 5.4$.

The linear function $H(z)$ provides a good fit to other sets of Hubble parameters (see [7, 11] for examples), except for the five-point compilation [11] obtained from the results of the DESI collaboration [12].

3 Photon number losses, the luminosity distance and the possibility to re-interpret the Hubble tension

In the model, the luminosity distance $D_L(z)$ is equal to:

$$D_L(z) = \frac{c}{H_0} \cdot \ln(1+z) \cdot (1+z)^{(1+b)/2}, \tag{3}$$

where b is the attenuation factor of the luminous flux caused by non-head-on collisions of photons with background gravitons [13, 7]. This factor was calculated for the case of a narrow beam of rays, when a photon after a collision leaves the photon stream registered by a remote observer [13]: $b = 2.137$. For photons with very high energy, $b = 0$ should be. But the exact dependence of b on the photon energy remains an open problem in the model. The dependence of the luminosity distance on the factor b, which can take different values for radiation sources with different spectra, makes the luminosity distance a multi-valued function of the redshift, which is very different from the situation in ΛCDM. This difference in models would be easy to detect by measuring the luminosity distances of distant sources of visible and gamma radiation, for example. Unfortunately, gamma-ray bursts (GRBs) have an unknown absolute luminosity, and they have to be calibrated in ΛCDM using supernovae.

Another open problem is a value of the photon energy by which we will have $b = 2.137$. Since b should increase with decreasing photon energy, this should

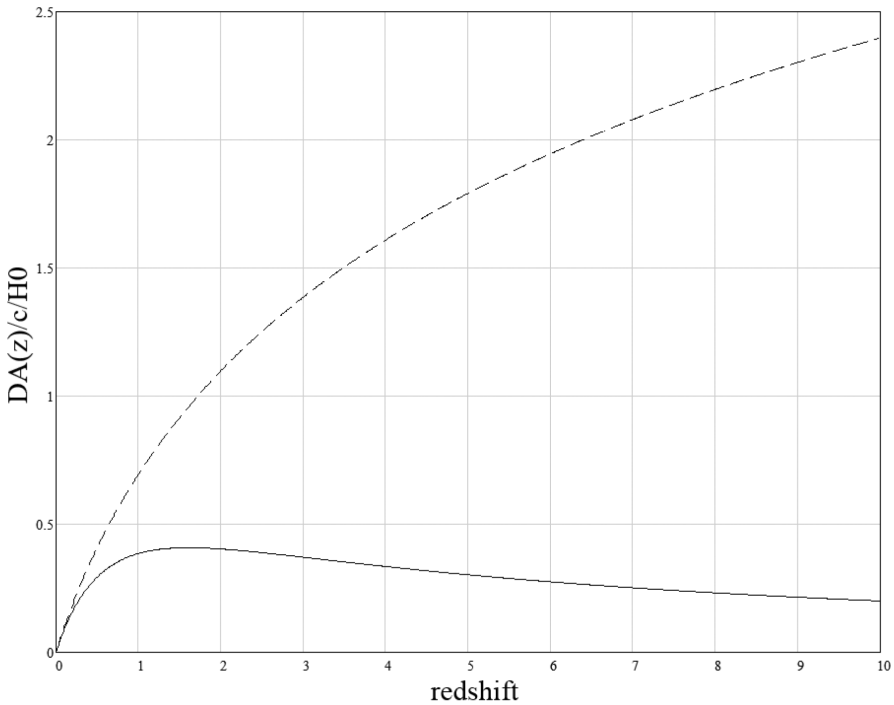

Figure 2: The angular diameter distance in unites of c/H_0 for a flat Universe with the concordance cosmology with $\Omega_M = 0.3$ and $w = -1$ (solid) and in this model without expansion (dash).

lead to some increase in b with increasing redshift if $b < 2.137$, i.e. to the replacement: $b \to b(z)$. If $b < 2.137$ in the ultraviolet, visible and infrared, this should lead to another observable effect - a change in the shape of the spectra of distant sources in these ranges. Spectral lines on the red side of the spectrum should be weakened more than lines on the blue side. It is possible that this putative effect leads to the appearance of small blue galaxies observed by JWST at redshift $z > 10$ [14, 15].

The ratio $\delta(z)$ of the scattered flux to the remainder that reaches the observer due to photon number losses is also determined by factor b [16]:

$$\delta(z) = (1 + z)^b - 1. \tag{4}$$

The possible formation of a background of visible radiation from these scattered photons may be related to the preliminary detection of a diffuse cosmic optical background by the New Horizons mission [17].

I want to demonstrate here that the possible dependence $b(z)$ allows for a different interpretation of the Hubble tension [18, 19]. If initially this term meant the detected difference between the locally measured value of H_0 and its value obtained by the Planck 2018 team [20] within a ΛCDM scenario (see Fig. 2 in [18]), now it is understood somewhat more broadly - as a change in the value of H_0 at different intervals of redshift values [21, 22]. In paper [21], the authors use the following phenomenological function $H_0(z)$ to obtain the best fit to the binned values of the Master sample of SNe Ia data: $H_0(z) = H_0'/(1+z)^\alpha$, where the parameters H_0' and α are evaluated.

Such a decrease in H_0 with increasing z in my model can be interpreted as an increase in b with increasing z at a constant H_0. To demonstrate the effect of such a change in b, I chose a linear trial function $b(z) = b_0 + a \cdot z$ and found the best values of H_0 for different values of its parameters b_0 and a when fitting $D_L(z)$ to the Union 2.1 compilation of SNe Ia [23]. The results are shown in Table 1; we see that the selection of the parameters of the trial function $b(z)$ allows us to reduce the estimate of H_0. Using function (3) with a constant $b = 2.137$ gives for the full data set: $< H_0 > \pm\sigma_0 = (68.22 \pm 6.10) km/s \cdot Mpc$, while dividing it into two subsets with $z < 0.15$ and $z > 0.15$ we have: $< H_0 > \pm\sigma_0 = (69.411 \pm 5.402) km/s \cdot Mpc$ for the first subset and $< H_0 > \pm\sigma_0 = (65.710 \pm 5.391) km/s \cdot Mpc$ for the second one [24].

b(z)	$< H_0 >$	σ_{H_0}
2.137+0.1z	68.454	6.002
2.137	68.223	6.097
2.0+0.1z	67.782	6.189
1.9+0.2z	67.526	6.233
1.8+0.24z	67,129	6.371
1.7+0.31z	66.805	6.477

Table 1: The linear functions $b(z)$ and the best fitting values of $< H_0 >$ and σ_{H_0} for the Union 2.1 compilation of SNe Ia from [23] corrected for no time dilation.

4 Model testability

The cosmic distance duality elation (CDDR):

$$\eta(z) \equiv \frac{D_L(z)}{D_A(z) \cdot (1+z)^2} = 1, \tag{5}$$

where $D_A(z)$ is the angular diameter distance, takes place under conditions: photon number is conserved, gravity is described by a metric theory and photons travelling on unique null geodesics [25]. While in [25] small deviations of $\eta(z)$ from 1 were reported caused by excess brightening of SNe Ia at $z > 0.5$, a recent paper [26] using reconstructed $D_L(z)$ from SN Ia and $D_A(z)$ from Megamaser data showed that CDDR holds in ΛCDM at $z < 0.04$, and using combining BAO and SN Ia data with appropriate choices of calibration parameters, that it holds at $0.04 < z < 1.6$. The authors of the paper [27] tested the performance of the CDDR using SNe Ia data (Pantheon data) and the compact radio quasars sample in the redshift range (0.4-2.26). In the paper [28] the measurement errors of $D_A(z)$ and $H(z)$ in the upcoming SPHEREx survey up to $z = 4.6$ are estimated in the ΛCDM model. Paper [29] describes observational tensions in cosmology, the ways to resolve them and the key objectives and potential new physics that may be observable in upcoming surveys.

This model differs significantly from the ΛCDM model. It is based on a non-metric gravity model, the number of photons in it changes due to scattering on

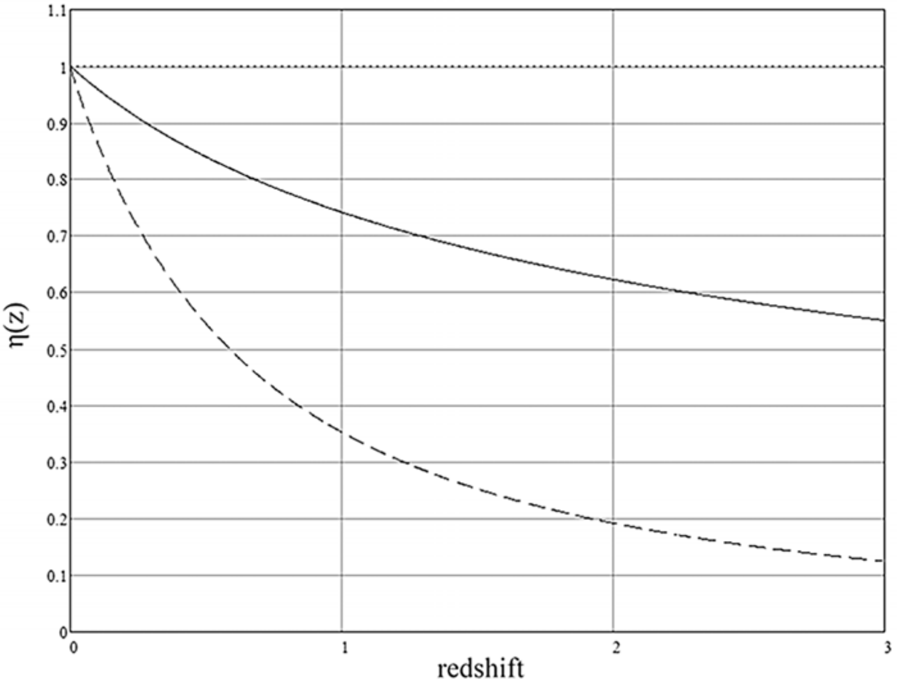

Figure 3: The graphs of functions (4) (dotted) and (5) with $b = 2.137$ (solid) and $b = 0$ (dashed).

gravitons, i.e. the attenuation of light from distant objects is not associated with dark energy, space is considered Euclidean, so the angular diameter distance $D_A(z) = r(z)$, there is no expansion of the Universe, and therefore there is no time dilation. If in the ΛCDM model the Hubble constant is a model parameter, then in this model it can be calculated. The functions $D_A(z)$ of the two models differ greatly, as can be seen in Fig. 2. If in ΛCDM $D_A(z)$ has a maximum at $z \approx 1.5$ and then monotonically decreases, in this model $D_A(z)$ is a growing function, which at $z = 10$ is almost 12 times greater than its analogue in ΛCDM. It may be that this is what leads to the apparent supercompactness of blue galaxies at $z > 10$ [14, 15]. Naturally, CDDR in the form $\eta(z) = 1$ does not take place. The theoretical expression for $\eta(z)$ has the form in this model:

$$\eta(z) \equiv \frac{D_L(z)}{D_A(z) \cdot (1+z)^2} = (1+z)^{(b-3)/2}. \tag{6}$$

This function may be equal to unity for all z, but with the value $b = 3$, which is unacceptable in this model. The graphs of functions (4) and (5) are shown in Fig. 3, and to compare the graphs of function (5) with the measurements, the $D_L(z)$ values must be corrected for no time dilation.

Using a data set of 120 milliarcsecond compact radio sources in quasars with the redshift range $0.46 < z < 2.76$ and with milliarcsecond angular sizes measured by very-long-baseline interferometry (VLBI), the authors of [30] in the ΛCDM model computed $D_A(z)$ for these sources and evaluated $< H_0 >$ to be $67.6 + 7.8 - 7.4$ km s-1 Mpc-1. The size of compact quasars was derived

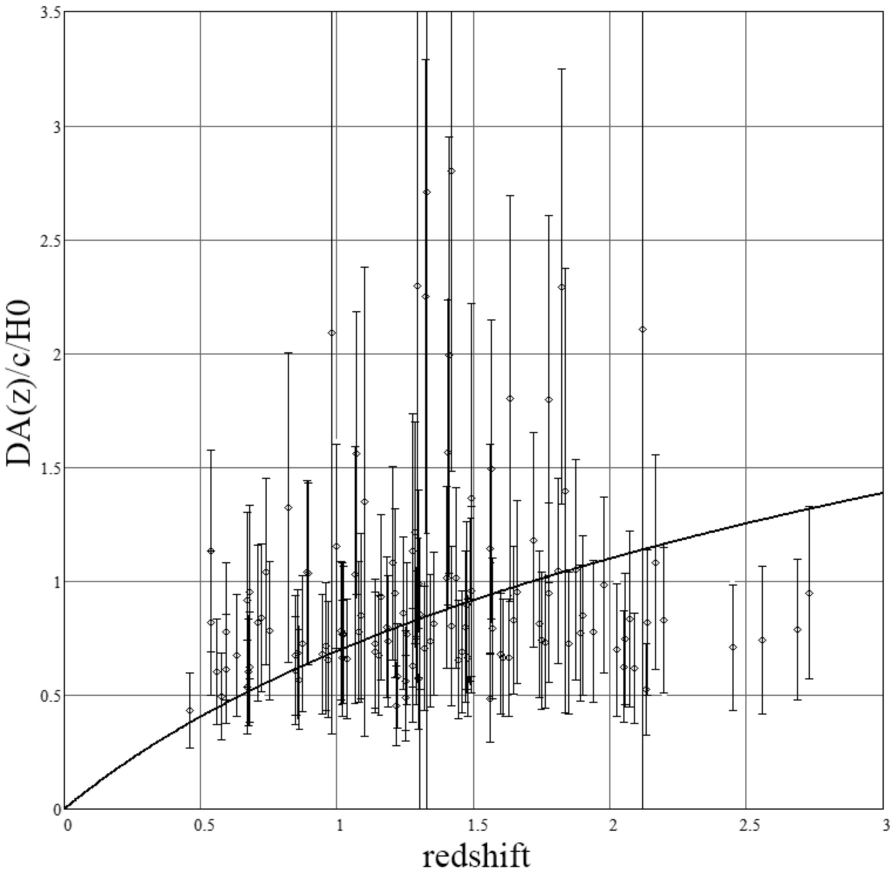

)

Figure 4: Plot of the theoretical angular diameter distance of this model (solid) and 120 angular diameter distance values calculated from the angular sizes of quasars taken from Table 1 of paper [30].

using a phenomenological model of a source and the observational $H(z)$ data: $l = (11.03 \pm 0.25)$ pc. The obtained values of the angular diameter distance are in agreement with the theoretical curve of the ΛCDM model with $\Omega_\Lambda = 0.7$.

In order to use the same data set of the angular sizes of compact quasars to fit the function $D_A(z)$ of this model, it is necessary to estimate the value of l independently of work [30]. To do this, I multiplied the measured values of the angles $\theta(z_i)$ from Table 1 of the article [30] by the values of the theoretical function $D_A(z)$ for the same z_i. Averaging over all points, I found the following estimate of l in $(c/H_0) \cdot milliarcsec$ units: $l = (1.187 \pm 0.458)$, or $l = (25.52 \pm 9.84)$ pc with $H_0 = 67.6$ km s-1 Mpc-1, which is approximately 2.3 times higher than the estimate of the cited work. This difference is due to the different scales of distances in the two models. Using this estimate, I calculated $D_A(z_i)$ using the formula: $D_A(z_i) =< l > /\theta(z_i)$ and found the standard deviation $\sigma_{D_A(z_i)}$ for indirect measurements of this quantity. The fitting results are shown in Fig. 4; in units of (c/H_0), the theoretical function $D_A(z)$ has no free parameters. The resulting value of $\chi^2 : \chi^2 = 98.247$ gives C.L. 91.75%. Changing the calibration of the linear size of distant objects increased the angular diameter distance values.

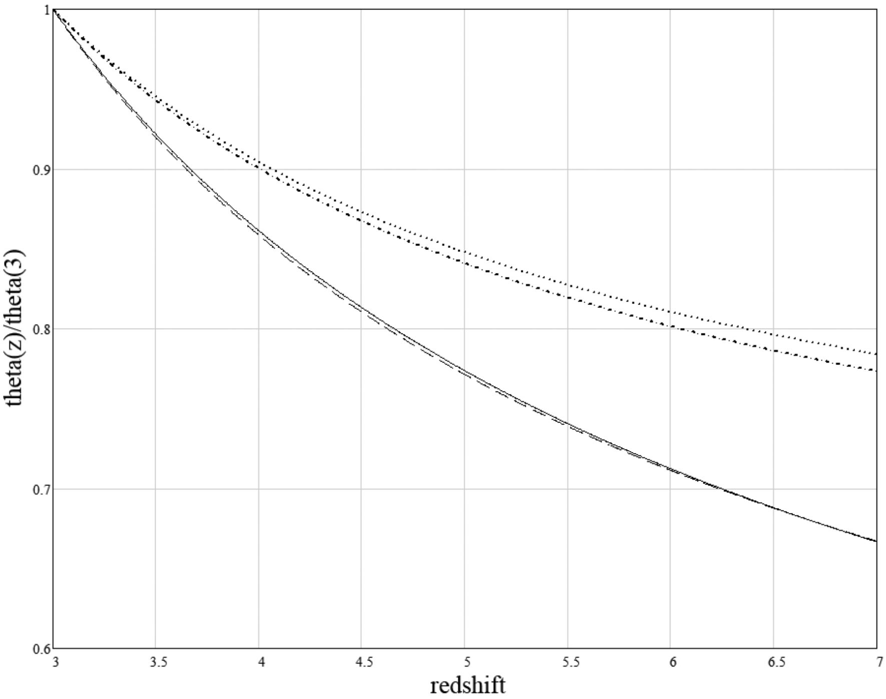

)

Figure 5: Graphs of the normalized functions $\theta(z)$ of this model for objects of constant linear size (solid) and functions of the form $\theta(z) \propto (1+z)^{\beta}/D_A(z)$ in the ΛCDM model with $\beta = \beta_0$ (dashed), $\beta =< \beta_1 >$ (dotted) and $\beta =< \beta_2 >$ (dash-dotted), the values of $< \beta_1 >$ and $< \beta_2 >$ are taken from article [31].

Perhaps measurements of the sizes of Lyman-alpha emitters with images from the James Webb Space Telescope (JWST) [31] are relevant to this topic. In this paper, analyzing a large sample of 876 spectroscopically confirmed Lyman-alpha sources at $3 < z < 7$, the authors found in the ΛCDM model a weak size evolution according to $\propto (1+z)^{-0.91\pm0.10}$ and $\propto (1+z)^{-0.93\pm0.18}$ in the rest-frame UV and optical ranges. To find the behavior of the measured angular sizes $\theta(z_i)$ of the emitters with changing redshift, I divided each of the two functions $(1+z)^{<\beta>}$ by the angular diameter distance $D_A(z)$ in the ΛCDM model with $\Omega_M = 0.3$. Since in my model the angular size of distant objects with constant linear size is proportional to $ln^{-1}(1+z)$, I also found a value of the exponent $\beta_0 = -1.143$, at which the function $(1+z)^{\beta_0}/D_A(z)$ in the ΛCDM model well models the function $ln^{-1}(1+z)$ of this model on the interval $z \in [3, 7]$. The graphs of these functions $\propto \theta(z)$, normalized to unity at $z = 3$, are shown in Fig. 5. We see that the graphs of $(1+z)^{<\beta_1>}/D_A(z)$ and $(1+z)^{<\beta_2>}/D_A(z)$ go above the graph of $ln^{-1}(1+z)$ for normalized functions, i.e. the size of the Lyman-alpha emitters from the point of view of this model rather increases with the growth of z. In units of standard deviations σ_β, the difference between the best value of β_0 for a constant emitter size and the values of $< \beta_1 >$ and $< \beta_2 >$ found in work [31] is $2.3 \cdot \sigma_{\beta_1}$ and $1.8 \cdot \sigma_{\beta_2}$ in the rest-frame UV and optical ranges, and here the errors in the absolute sizes of the emitters for $z = 3$ were not taken into account.

5 Conclusion

The difference in paradigms on which this model and the ΛCDM model are based must be taken into account when comparing the theory with the measurement results. The measurements of the luminosity distance must be corrected for no time dilation in this model. The angular diameter distance should be found with different calibration of the linear size of distant objects. It is important to explore the possible confounding of the influence of evolution on the apparent size of an object and its dependence on the angular diameter distance. The Hubble parameter $H(z)$ in this model has no connection with the history of cosmological expansion, the Hubble constant describes the energy loss of photons when passing through the graviton background. The set of small effects described in the article is already partially observed, but has a different interpretation; the rest can be discovered with closer attention. As shown here, the dependence of the attenuation factor b on the photon energy can lead to a different interpretation of the Hubble tension. The possible formation of a background of visible radiation in the model, presumably detected by the New Horizons mission [17], requires additional study by future deep space missions.

References

[1] Amendola, L., Tsujikawa, S. 2010. Dark Energy: theory and observations. Cambridge University Press. https://doi.org/10.1017/CBO9780511750823.

[2] Bhattacharjee, S., Halder, S., Haro, J. de, Pan, S., Saridakis, E.N. (2025). Accelerating Universe without dark energy: matter creation after DESI DR2. arXiv:2507.15575v1 [astro-ph.CO].

[3] Sadoulet, B. (2024). Forty years of dark matter searches. Nuclear Physics B, 1003, 116509. https://doi.org/10.1016/j.nuclphysb.2024.116509.

[4] Ishak, M., Medina-Varela, L. (2025). Is this the fall of the ΛCDM throne? Evidence for dynamical dark energy rising from combinations of different types of datasets. arXiv:2507.22856v1 [astro-ph.CO].

[5] Wang, J., Yu, H., Wu, P. (2025). Revisiting cosmic acceleration with DESI BAO. arXiv:2507.22575v1 [astro-ph.CO].

[6] Amelino-Camelia, G. (2002. Quantum-gravity phenomenology: status and prospects. Mod. Phys. Lett. A 17, 899-922. https://doi.org/10.1142/S0217732302007612.

[7] Ivanov, M.A. (2018). Selected papers on low-energy quantum gravity. http://ivanovma.narod.ru/selected-papers-Ivanov2018.pdf.

[8] Ivanov, M.A. (2024). Superstrongly interacting gravitons: low-energy quantum gravity and vacuum effects. *Horizons in World Physics*. Volume 312; Reimer, A. (Ed.); Nova Science, NY, 225-240.

[9] Ivanov, M.A. (2025). Gravity as a screening effect. Current Physics, 2, e27723348373429. https://doi.org/10.2174/0127723348373429250512104534.

[10] Moresco, M., Amati, L., Amendola, L. et al. (2022). Unveiling the Universe with emerging cosmological probes. Living Rev Relativ 25, 6. https://doi.org/10.1007/s41114-022-00040-z.

[11] Ivanov, M.A. (2024). Quantum gravity without quantization. Current Physics **1**, e27723348344123. https://doi.org/10.2174/0127723348344123241030061731.

[12] DESI Collaboration: Adame, A.G., Aguilar, J., Ahlen ,S., S. Alam, S., Alexander, D. M. et al. (2024). DESI 2024 VI: Cosmological Constraints from the Measurements of Baryon Acoustic Oscillations. arXiv:2404.03002v2.

[13] Ivanov, M.A. (2004). Another origin of cosmological redshifts. arXiv:astroph-0405083.

[14] Ziparo, F., Ferrara, A., Sommovigo, L., Kohandel, M. Blue monsters. (2023). Why are JWST super-early, massive galaxies so blue? Monthly Notices of the Royal Astronomical Society, 520(2), 24452450. https://doi.org/10.1093/mnras/stad125

[15] Lei, L. et al. (2025). Stringent constraint on the CCC+TL cosmology with $H(z)$ measurements. arXiv:2508.04277v1 [astro-ph.CO].

[16] Ivanov, M.A. (2024). Three Different Effects of the Same Quantum Nature. PoS(EPS-HEP2021)114.

[17] Lauer, T.R., Postman, M., Weaver, H.A., Spencer, J.R. et al. (2021). New Horizons Observations of the Cosmic Optical Background, Astrophys. J., 906, 77. https://doi.org/10.3847/1538-4357/abc881

[18] Valentino, E. Di et al. (2021). In the realm of the Hubble tension a review of solutions.Class. Quantum Grav. 38(15), 153001. https://doi.org/10.1088/1361-6382/ac086d

[19] Riess, A.G. et al. (202). A comprehensive measurement of the local value of the Hubble constant with 1 km s^{-1} Mpc^{-1} uncertainty from the Hubble space telescope and the SH0ES team. ApJL, 934, L7. https://doi.org/10.3847/2041-8213/ac5c5b

[20] Aghanim, N., Planck et al. (2020). Planck 2018 results. VI. Cosmological parameters. Astron. Astrophys., 641, A6. https://doi.org/10.1051/0004-6361/201833910

[21] Dainotti, M. G. et al. (2025). A New Master Supernovae Ia sample and the investigation of the H_0 tension. arXiv:2501.11772v5 [astro-ph.CO].

[22] Montani, G., Fazzari, E., Carlevaro, N., Dainotti, M.G. (2025). Two dynamical scenarios for the binned Master sample interpretation. arXiv:2507.14048v1 [astro-ph.CO].

[23] Suzuki, N., Rubin,D., Lidman, C., Aldering, G., Amanullah,R., Barbary, K., ... & Supernova Cosmology Project. (2012). The Hubble Space Telescope Cluster Supernova Survey: V. Improving the Dark Energy Constraints Above $z > 1$ and Building an Early-Type-Hosted Supernova Sample. Astrophys. J., 746, 85. https://doi.org/10.1088/0004-637X/746/1/85

[24] Ivanov, M.A. (2025). The interaction of photons with the graviton background and cosmological observations. https://vixra.org/pdf/2505.0199v1.pdf.

[25] Bassett, B.A, Kunz, M. (2004). Cosmic distance-duality as probe of exotic physics and acceleration. Phys.Rev., D69, 101305. https://doi.org/10.1103/PhysRevD.69.101305. arXiv:astro-ph/0312443v2

[26] Kanodia, B., Upadhyay, U., Tiwari, Y. (2025). Revisiting Cosmic Distance Duality with Megamasers and DESI DR2: Model Independent Constraints on Early-Late Calibration. arXiv:2507.11518v1. [astro-ph.CO].

[27] He, Y. et al. (2022). Cosmological-model-independent tests of cosmic distance duality relation with Type Ia supernovae and radio quasars. Chinese Journal of Physics, 78, 297-307. https://doi.org/10.1016/j.cjph.2022.06.009. arXiv:2206.04946v1 [astro-ph.CO]

[28] Roman, A.M., Ocampo, I., Nesseris, S. (2025). Forecast constraints on null tests of the ΛCDM model with SPHEREx. arXiv:2507.16604v1 [astro-ph.CO].

[29] Valentino, E. Di et al. (2025). The CosmoVerse White Paper: Addressing observational tensions in cosmology with systematics and fundamental physics. arXiv:2504.01669v2 [astro-ph.CO].

[30] Cao, S. et al. (2017). Ultra-compact structure in intermediate-luminosity radio quasars: building a sample of standard cosmological rulers and improving the dark energy constraints up to $z \sim 3$. A&A, 606, A15. https://doi.org/10.1051/0004-6361/201730551. arXiv:1708.08635v1 [astro-ph.CO]

[31] Song, Q. et al. (2025). The size evolution and the size-mass relation of Lyman-alpha emitters across $3 < z < 7$ as oObserved by JWST. arXiv:2508.05052v1.